ORIGINAL ARTICLE

lajss.org© Latin American Journal of Solids and Structures

www.lajss.org

Effect of axial and rotational restraint on performance of composite beams with fire protection coating

Igor Charlles Siqueira Leite[a]*, Valdir Pignatta Silva[b]

[a]Departamento de Engenharia de Estruturas e Geotecnica, Av. Prof. Almeida Prado, trav.2 n. 83 Cidade Universitaria, São Paulo, 05508-900, São Paulo, Brasil. E-mail: igorleite@usp.br
[b]Departamento de Engenharia de Estruturas e Geotecnica, Av. Prof. Almeida Prado, trav.2 n. 83 Cidade Universitaria, São Paulo, 05508-900, São Paulo, Brasil. E-mail: valpigss@usp.br

* Corresponding author

https://doi.org/10.1590/1679-78257403

Abstract

This paper presents the behavior of steel-concrete composite beams with fire protection using the finite element software ABAQUS. An extensive parametric study was carried out to verify the influence of the axial and rotational restraint stiffness, the influence of the spans and the influence of the variation of the fire protection coating, topic with few studies by other authors. The focus of this paper was to verify the axial forces on the supports to study the influence of these forces on the surrounding elements: columns and connections. The study shows that axial and rotational constraints have an important influence on the beams. The values of axial forces are proportionally greater as the beam span is increased. Also verified was that the beam behavior does not change with the variation of the fire protection coating. Finally, the study brings a new approach to the importance of investigating the forces of interaction between beams and columns, as theses forces can lead to unsafe design because the compressive forces in the interaction with the columns and the tensile forces in the catenary phase in connections.

Keywords

Fire Engineering; Restrained Composite Beam; Fire Protection

Graphical Abstract

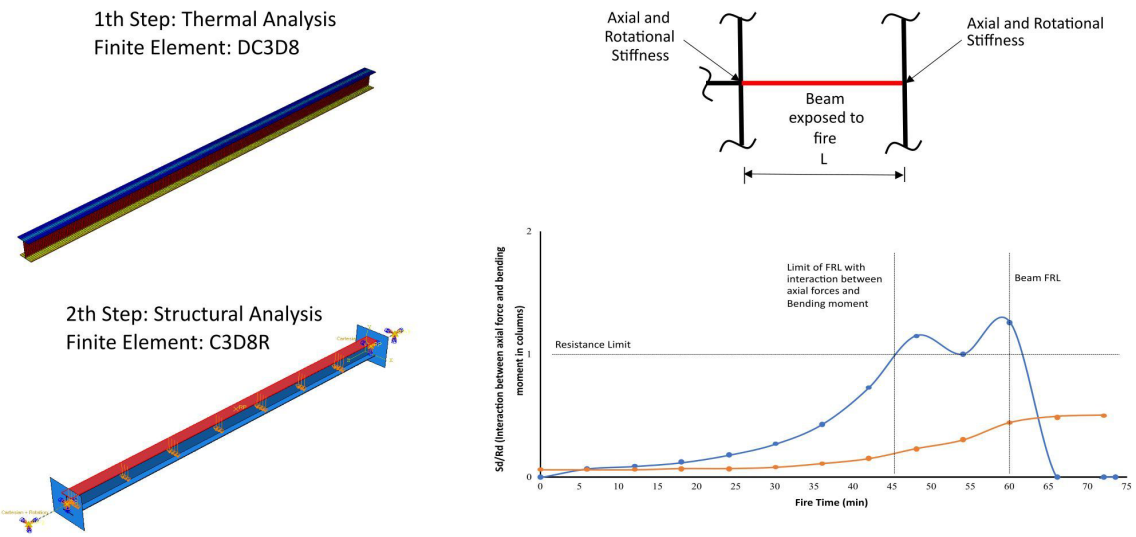

Received: December 05, 2022. In revised form: February 10, 2023. Accepted: March 07, 2023. Available online: March 16, 2023.
https://doi.org/10.1590/1679-78257403

Latin American Journal of Solids and Structures. ISSN 1679-7825. Copyright © 2023. This is an Open Access article distributed under the terms of the Creative Commons Attribution License, which permits unrestricted use, distribution, and reproduction in any medium, provided the original work is properly cited.

1 INTRODUCTION

The behavior of simply supported beams is relatively simple to investigate. Silva (1997) studied the behavior of these types of beams, verifying that, in a fire situation, the beam initially has a constant vertical displacement; later, with the degradation of the mechanical properties at high temperatures, the beam shows a large deflection until reaching the its critical temperature, which is the formation of plastic hinges in the center of the span. The load capacity of a simply supported beam is based on the region under the maximum bending moment, when it reaches the plastic capacity of the beam (Najafi, 2014). The critical temperature is a function of the beam load ratio, that is, the relationship between the load applied in a fire situation and the load associated with the total plastification moment of the beam at room temperature.

Regarding the support conditions of beams, when they are part of a frame, or rather, when they are supported on vertical elements (usually columns), beams have axial or rotational restrictions at their ends that can act together. Note that, in design situations, the beams always have axial restrictions, obviously varying the value of their stiffness. Figure 1 allows verifying the beam model with axial and rotational constraints.

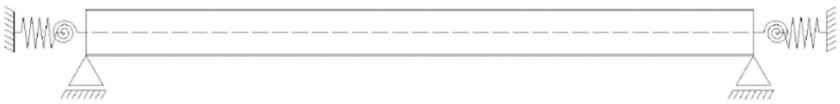

Figure 1 Beam model with axial and rotational restraint.

The simple fact that the beam has a stiffness in its support allows this element to behave in a very different way from when it has support without axial restriction. Wang (2002) provides an explanation of this behavior, summarized in Figure 2. At first, the beam axial restraint causes the thermal expansion to be restrained, and this expansion is transformed into an axial compression force at the support. The unrestricted portion of the thermal expansion will increase the length of the beam. When the bending moment and compressive force are adequately high, they can cause local instability near the ends of the beam (Leite and Silva, 2021). Then, as the temperature in the structural element increases, both the bending moments and the compressive forces decrease in value.

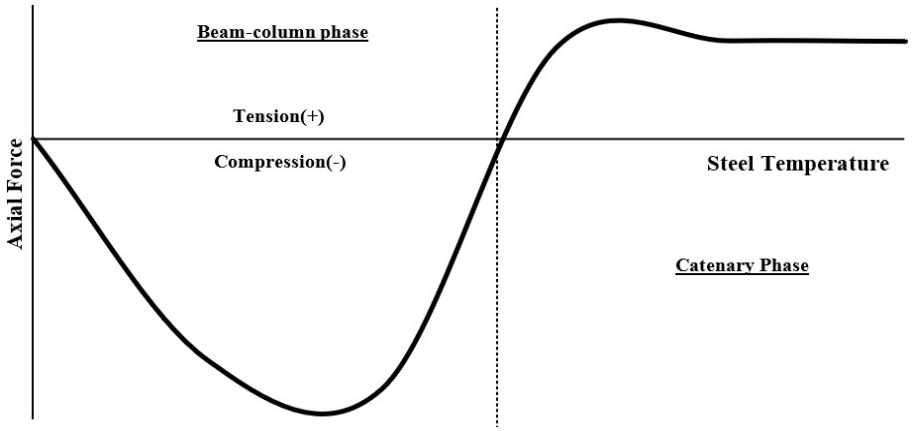

Figure 2 Axial force response of a restrained steel beam exposed to fire.

In the catenary phase, the tensile forces develop in the beam up to a maximum value; it is thus possible to verify the plastification of the section in the middle of the span and in the supports of the beam (Usmani *et al*, 2001). The catenary model assumes that the steel beam, when heated, works as a cable that supports the structure around it (which is not heated); however, due to the high temperature in the beam, the mechanical properties are reduced. This model is used to calculate the relationship between the midspan displacements and the axial tensile force to which it is associated in a fire situation. The reduction of the resistance capacity of the beam, in combination with the internal forces that appear due to the restrictions to displacements, make the behavior of the beam in a fire situation completely different from the behavior at room temperature (Kodur and Dwaikat, 2009).

In the early stages of heating, the structure around the beam tends to resist the thermal expansion. The vertical displacements of the beam are increased by this expansion, along with the thermal deformation resulting from

temperature variation along the beam cross section. Since the thermal properties of steel degrade rapidly at temperatures above 350°C, the beam shows large deformations depending on the level of loading applied (Allam *et al*, 2002). However, the large deformations in the beams can be attenuated from the point where it behaves as a cable, since the support structure is able to redistribute the efforts and resist the beam at high temperatures with the level of loading during the fire.

If the beams are connected to columns with low flexural resistance, they will need to resist forces due to the catenary action of the beams, and thus the resistance of the columns command the design. According to Wang (2002), the columns will need to be dimensioned for a greater capacity of bending moment. In this case, catenary action can be used to avoid the progressive collapse of the structures, since the more rigid column allows the catenary action helping to release the excessive vertical displacements. However, tensile forces in the catenary action can lead to connection failure (Chen and Wang, 2012). The support conditions of the beam providing varying levels of axial and rotational restraint. The internal forces for different levels of restraint are dependent on the stress-strain relationship of the steel in fire situation. In addition to the aforementioned effects, local buckling occurs in the beams due to the thermal expansion in the axially restrained beams, which can cause the fire insulation to be destroyed. Tensile stresses during catenary action can cause tensile cracks in concrete slabs (Martinez and Jeffers, 2021).

In recent works, Selden and Varma (2016) studied the behavior of composite beams in fire situations using numerical models with the ABAQUS software (Dassault, 2018), where the authors were able to identify failure models of composite beams, including failure by compression in the concrete slab, the runaway deflection of the steel beam and the fracture of the shear studs. However, this study did not consider different levels of axial and rotational restraint at the supports. Guo et al. (2018) derived equations to predict the limit state of restrained steel beams in fire situation, using reduction factors of elastic modulus and yield strengths. The presented equations provide values such as maximum compressive forces, maximum catenary tensile forces and span/20 of mid-span deflections. However, the study was limited to the development of analytical equations without incorporating numerical modeling. The behavior of axially restricted beams was studied by Allam et al (2019) using computational methods, to investigate how the surrounding structures affect the survival of steel framed structures in fire. Other work included numerical studies of composite steel and concrete beams subjected to fire under different support conditions (Romagnoli and Silva, 2020). In this work, the authors compared the results found with the simplified design methods recommended by the main codes on steel structures in fire situations.

Although the behavior of restrained composite beams in fire situation has been widely studied, no work presents a parameterization of different types of fire protection material to study the beam behavior and there is also no focus on the interaction between the effects caused by the axial and rotational constraints of the beams on the surrounding elements. Although the European Code (EN 1993-1-2, 2005) establishes that the interactions between the structural elements must be analyzed, it is unclear whether the compressive and tensile forces, caused by expansion and catenary action, respectively, can be neglected in the design of isolated elements. In order to investigate the aforementioned behavior, this work investigates the behavior of composite beams with axial and rotational restrictions, verifying the influence of the variation of the beam span, the variation of the axial and rotational restriction level and the variation of the fire protection materials, mainly for analyzing whether the compressive force during the expansion phase and tensile forces during catenary action influence the adjacent structural elements, particularly the columns and beam column connections, using the finite element software ABAQUS (Dassault, 2018). In addition, the results presented are based on the fire time and not on the temperature in the element, since the mair purpose of the fire coating is to delay the degradation of the mechanical properties of the material.

2 DESCRIPTION OF NUMERICAL MODELS

2.1 General aspects of thermostructural analysis

The numerical models here in were developed in the finite element software ABAQUS. The analysis is divided into two steps. The first step is the thermal analysis to predict member temperatures, while the second step is the coupled structural analysis, using the results found in the thermal analysis from the Predefined Fields option (Figure 3). Note that the solver chosen for the coupled structural analysis is Dynamic/Explicit. ABAQUS reduces possible dynamic noise and enhances convergence performance using numerical energy dissipation in its solver. The finite element used for modeling the thermal analysis was the DC3D8 type, a three-dimensional element with 8 nodes. The finite element used for modeling the thermostructural analysis was the C3D8R type, a three-dimensional linear element with 8 nodes, with only one integration point, since this element promotes a reduced time for the analysis at high temperatures. The thermal

properties of steel and concrete were defined from the provisions of ABNT NBR 14323 (2013) and ABNT 15200 (2012), respectively. The temperature-dependent thermal properties of fire protection materials (SFRM CACFO-300 and Carboline Type, square edged gypsum board and intumescent paint) were taken from numerical and experimental studies (Kodur and Shakya, 2013), (Rigobello, 2011) and (Krishnamoorthy, 2011), respectively. The fire protection coating was modeled as a solid element (DC3D8) only in thermal analysis. In the thermostructural analysis, only the predefined temperature distribution in the steel beam from the previous step was considered. Some thermal analysis model of composite beams with fire protection coating can be seen in Figure 4. The heating was applied to the bottom face of the concrete slab and all the faces of the steel profile, except the steel profile upper face, which is in contact with de concrete slab. The room temperature starts at 20°C. The alfa convection heat transfer coefficient was considered constant and equal to 25W/m^2.C. An emissivity of ε_r = 0.7 was used to define the radiation conditions prescribed in ABNT NBR 14323 (Associação Brasileira de Normas Técnicas, 2013). The thermal expansion coefficient was taken as 0.000014/°C in the models of this paper, except in the validation of results in that used different values from those considered in this paper.

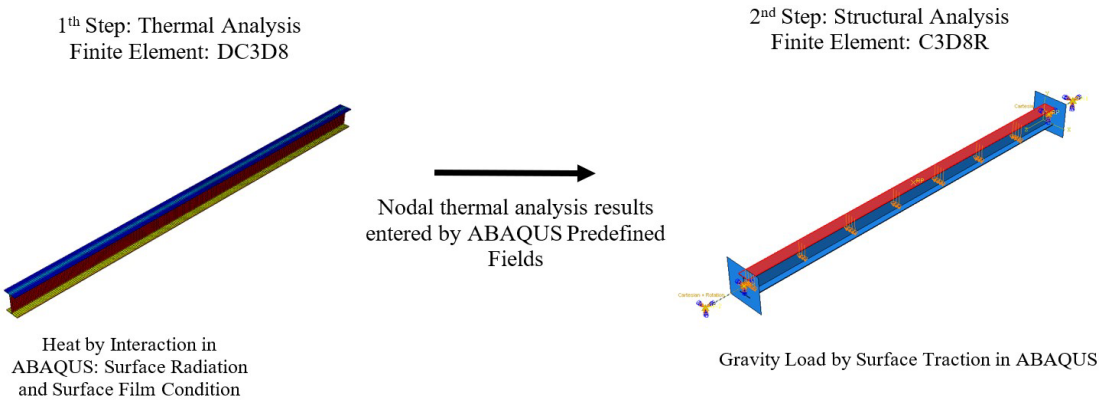

Figure 3 Schematic representation of loads applied in the thermostructural model

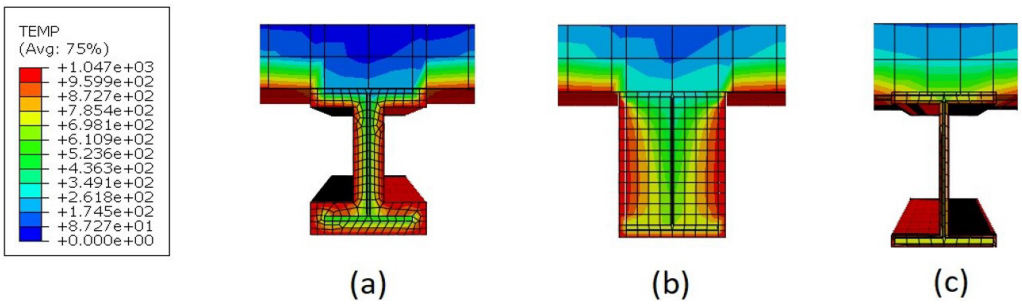

Figure 4 Thermal analysis model of composite beams with fire protection coating: (a) SFRM; (b) square edged gypsum board; (c) intumescent paint

The nonlinearity of the material was established by the stress-strain diagram provided in Eurocode Part 1-2 (11). Geometric nonlinearity is incorporated into the model by selecting the "NLGEOM" option in the ABAQUS Explicit solver. The boundary conditions used in the simulations of this paper are represented in Figure 5. Rigid plates were fixed to the ends of the beam. The connection of the plates to the beam was made using the coupling constraint option of ABAQUS. To simulate the axial and rotational stiffness of the models, respectively, a connection element "CONN3D2" was used, which behaves as a spring due to the stiffness properties entered in the connector section field. The wire element is connected to two points of the model: a point connected to the centroid of the plate and another point at a position away from the beam. A boundary condition is applied to the first point to release axial and rotational deformations. At the second point, a fixed end type boundary condition is applied, restricting all the movements. This artifice is necessary for the analysis to converge without stability problems. The stiffness of the springs was assumed not to be affected by temperature. This scenario assumes that the joint region (column and connection) has been protected from fire.

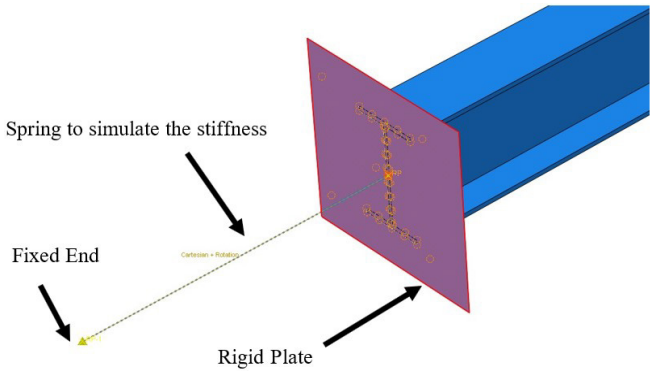

Figure 5 Boundary conditions of the numerical simulation beams

2.2 Validation of numerical models

The numerical model was compared to a series of fire tests. The validation was divided into two parts. The first part demonstrates the validation of a restrained steel beam, according Liu et al (2002) fire test. The numerical results obtained by Yin and Wang (2004) and Najafi (2014) will also be used in the validation. The second part demonstrates the validation of a simply-supported steel-concrete composite beam, according to Wainman and Kirby (1987) standard fire test.

Liu et al (2002) performed a series of tests to study the effects of axial and rotational restraint on beams at high temperatures. The profile used is UB178x102x19, S275 steel grade (f_y = 275 MPa), span of two meters, and two concentrated loads, with a rate of 0.5 and 0.7 of the ultimate load at room temperature. The values are 38.3 kN and 52.6 kN, respectively. In the numerical model, these loading was applied to an area equal to the width of the flange to avoid numerical errors in the analysis. The axial stiffness considered was 8 kN/m and the rotational stiffness was estimated as 14000 kNm/rad. The estimate was made because this value was not present in the work by Liu et al (2002). In Figure 6 depicts the correlations between experimental data and numerical analysis, including models from other authors.

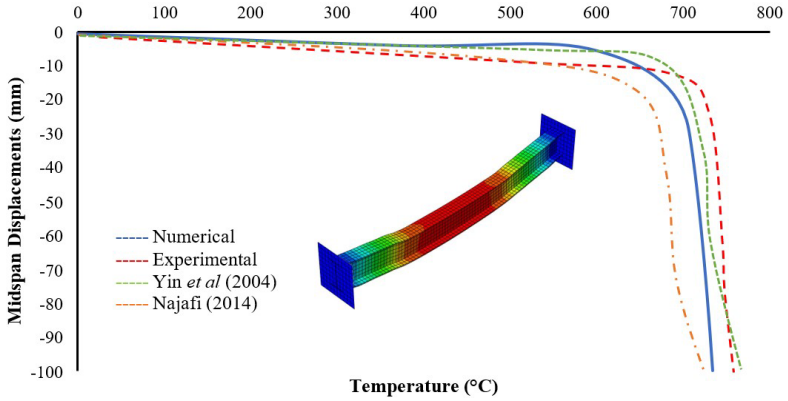

Figure 6 Correlations between experimental data and numerical analysis

Based on the results presented in Figure 6, the values found in this work are slightly more conservative than those found by Najafi (2014) and Yin and Wang (2004). However, both works have the same initial stiffness, showing the same displacements up to approximately 200°C. This difference is because different values are being used in relation to the yield stress, as explained in Yin and Wang (2004).

Regarding the for validating of composite beam models, the experimental data found by Wainman and Kirby (1987) is used. The authors in question performed several tests in Rotherham, England, to evaluate the behavior of uncoated steel and concrete composite beams in fire situation. Fire Test 15 of those authors was chosen for validating the models used herein. The choice for this test was given by the similarity of what is used in the models of composite beams in this paper. Test 15 analyzed a British steel profile UB 254 x 146 x 43 that was connected to a reinforced concrete slab using stud bolts. The total span of the beam is 4350 mm. The slab has a width of 642 mm and a thickness of 130 mm. The slab reinforcement has a diameter of 8 mm spaced 200 mm longitudinally and 100 mm transversely. The shear connectors are spaced 95 mm apart in two rows on the top flange of the beam with a distance 280 mm between the connectors, with a diameter of 19 mm. The profile steel yield strength is equal to 280 MPa. In Test 15, four concentrated loads of 32.5 kN were applied. The oven heating followed the curve defined in BS 476:1972 – Part 8, like ISO 834 curve. The concrete has a compressive strength

of 30 MPa. Cedeno et al (2011) performed the validation of their numerical modeling also based on the work by Wainman and Kirby (1987), emphasizing that these tests were carried out up to 40 minutes of fire, that is, results were not measured after that time. The results found by Wainman and Kirby (1987) and Cedeno et al (2011) and those found in this paper can be seen in Figure 7. The numerical result is verified to present good results with the test data, showing that the numerical model can be used to capture the fire responses of composite beams.

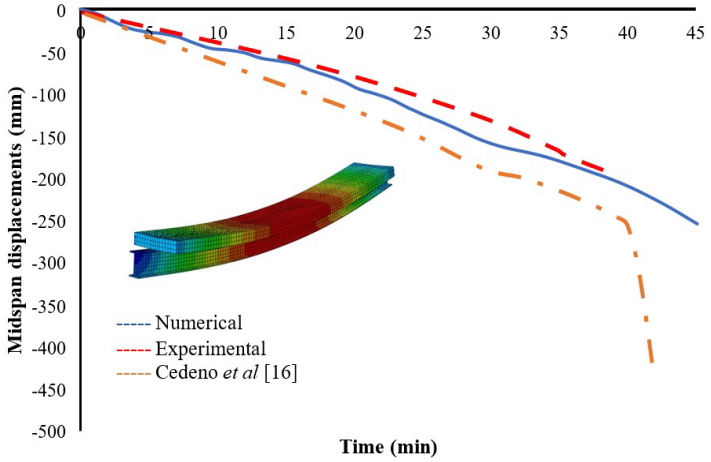

Figure 7 Numerical model compared to Fire Test 15 results

3 PARAMETRIC STUDY OF COMPOSITE STEEL AND CONCRETE BEAMS WITH AXIAL AND ROTATIONAL CONSTRAINTS WITH FIRE PROTECTION COATING

In this parametric study, spans of 5, 10 and 15 meters were studied, with brazilian welded profiles VS 350x25, VS 500x73 and VS 700x154, for each span, respectively. Table 1 shows the geometric characteristics of the profiles chosen. It was decided that the beams under study are parts of a frame, whose distance between the beams and columns outside the plane is 5 meters. The profiles were chosen based on the smallest possible cross-section for each adopted span, using a dead load of 1 kN/m^2 and live load of 5 kN/m^2. The combinations of actions were carried out according to what is prescribed in ABNT NBR 8800 (Associação Brasileira de Normas Técnicas, 2008). The steel class adopted is ASTM A36 with 250 MPa yield strength and 400 MPa ultimate strength. The load applied to the beam is of the order of 0.4 of the maximum composite beam loads at room temperature considering a beam fixed at both ends. The reinforced concrete slabs were designed by ABNT NBR 6118 (Associação Brasileira de Normas Técnicas, 2014). The stud bolts were dimensioned based on the criteria of ABNT NBR 8800 (Associação Brasileira de Normas Técnicas, 2008). This parametric study simulated the behavior of composite beams in a substructure as if the beam were connected to a perimeter column at the right support and an intermediate column at the left support.

Table 1 Steel profile parameters

Profile	d (depth)	b_f (width)	t_f (thickness)	t_w (thickness)
VS 350x25	350 mm	140 mm	6.3 mm	4.75 mm
VS 500x73	500 mm	250 mm	12.5 mm	6.3 mm
VS 700x154	700 mm	320 mm	22.4 mm	8.0 mm

The beam is heated by the three lower faces and the slab is heated by the lower face, simulating a fire in a building. Concrete with the characteristic compressive strength, fck, equal to 30 MPa was assumed. The slab was reinforced with a CA-50 steel bars (f_y = 500 MPa) located 30 mm from the bottom of the slab. ASTM A36 steel (f_y = 250 MPa) was considered for the stud bolts. For modeling the slabs, the plasticity damage of concrete (Jankowiak and Lodygowski, 2005) was implemented to represent the elastoplastic behavior of concrete, using concepts of isotropic elasticity and compressive plasticity. The high temperature mechanical properties of steel, including the modulus of elasticity and plasticity, were obtained from ABNT NBR 14323 (Associação Brasileira de Normas Técnicas, 2013). The fire protection materials used were spray applied fire resistive material (SFRM) CACFO-300 and Carboline Type, intumescent paint, and square edge gypsum board. The interaction between fire protection materials and steel beams is accounted for by the

"Tie" constraint in ABAQUS, while the interaction between reinforcements, stud bolts and the concrete slab is defined by the "Embedded Region" constraint. The beams were vertically loaded on the upper face of the concrete slab, in the region above the steel beam top table, with distributed loading. Figure 8 shows the model of steel and concrete composite beam used. The parameters to be considered in the parametric analysis are: Beam length (L); Axial constraint level (Ka); Rotational Restriction Level (Kr) and Fire Protection Materials. The axial restraint values used were: Ka = 0.05KA, Ka = 0.1KA, Ka = 0.5KA and Ka = KA. The rotational constraint values used were: Kr = 0.05KR, Kr = 0.1KR, Kr = 0.5KR, Kr = KR and Kr = KRI (infinite rotational constraint). Being KA and KR taken respectively as EA/L and 2EI/L, where E is the Young´s modulus of steel at 20 °C, A is the cross-sectional area of the steel profile, L is the span length of the beam and I is the moment of inertia in the major axis. The load factor used is 0.4, definied over the nominal bending moment of the composite beam. Table 2 shows the parameters of the investigated cases.

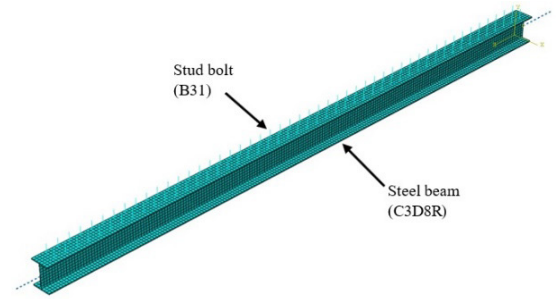

(a) FE modeling of steel beam and stud bolts

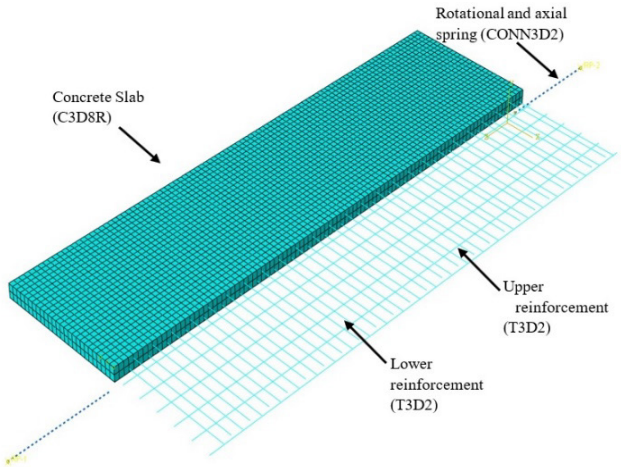

(b) FE modeling of steel reinforcement, concrete slab and rotational and axial spring

Figure 8 Uncoated steel and concrete composite beam model

Table 2 Investigated cases in the parametric study

Model	Profile	Spam	Failure load at room temperature	Loat at Fire Situation	KA	KA
		m	kN/m	kN/m	kN/m	kN.m/rad
VM1	VS350x25	5	81.18	32.4	130800	5384
VM2	VS500x73	10	78.42	31.3	184800	17107.2
VM3	VS700x154	15	92.8	37.1	261067	48898.1

The fire protection materials used in this parametric study are specified in Table 3, with the respective nomenclature used and their thicknesses. The thicknesses were chosen based on the mass factor of the beam, so that, in 120 minutes in the thermal analysis via FEM, the steel beams had approximately the same temperature as that at the end of the fire. The models in the parametric analysis considered the model, span and level of axial and rotational restriction and respective fire protection material. For example, model VM-5-0.5KA-KR-TI represents a VS 350x26 profile beam, 5-meters span, 50% of axial restraint, full rotational restraint, with intumescent paint as a fire protection material.

Table 3 Fire protection coating materials investigated in the parametric study

Initials	Fire Coating	Thickness
APCa	CACFO 300	25.4 mm
APCr	Carboline	25.4 mm
PGA	Gypsum Board	12.5 mm
TI	Intumescent Paint	5 mm

A mesh study was carried out in ABAQUS to verify by how much the finite element mesh refinement influences the structural response of the models. For steel beams, the mesh size of 15 mm presented significant results with less computational resources. For the concrete slab, three meshes were evaluated, as presented in Table 4. It was observed that Mesh 1 required approximately 1.5 times more time to complete the analysis (182 min) compared to Mesh 2 (123 min). Despite both meshes having a relatively long analysis time, they demonstrate the effect of incorporating the plasticity damage properties of the concrete. Figure 9 demonstrates that Mesh 2 has an appropriate size, as it exhibits minimal variations in terms of displacement and critical temperature (Span/30) compared to other refined meshes. Based on these findings, Mesh 2 was selected for the reinforced concrete slabs in this study. An important consideration in the modeling was that the slab cannot be discretized with only one element in its thickness. The elements of type C3D8R (reduced integration) of ABAQUS admit constant deformation in their domain, having only one Gauss point and, if there was only one element, the Gauss point will be on the neutral line of the slab, causing the element to lose its bending stiffness. Therefore, the slab must have at least two elements in its thickness.

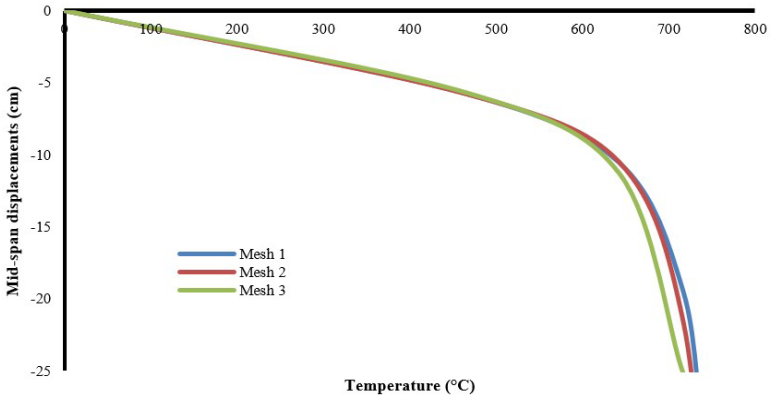

Figure 9 Refinement analysis of the finite element mesh of the concrete slab

Table 4 Critical temperature of composite beam from finite element mesh refinement

Mesh reference	Slab Mesh Refinement	Critical Temperature	Analysis Time
	m	°C	min
1	0.025	728	182
2	0.05	730	123
3	0.075	732	104

3.1 Parametric analysis results

3.1.1 Influence of the axial and rotational stiffness

The results found for the SFRM Carboline Type present the variation of the axial stiffness on the fire-coated beams. In the analyses, negative forces correspond to compressive axial forces and positive forces correspond to tensiles axial forces. Figure 10 show that, as the level of axial stiffness decreases, the compressive forces on the supports also decrease, causing the beam displacements in the center of the span to also decrease. The explanation is that, with less axial constraint, the beam presents a greater horizontal displacement due to thermal expansion, reducing the vertical displacements and, because of the little constraint to the horizontal displacement, the axial support reactions have

reduced values. Also noteworthy is that the fire time in which the values of the maximum reactions occur varies according to the level of axial restraint. This consideration is important, especially in the design of the elements surrounding the beam. Still on the axial forces in the supports, the presence of tension forces was not verified in the models with SFRM Carboline type. However, in the other models studied, tensile forces in the catenary phase can be observed.

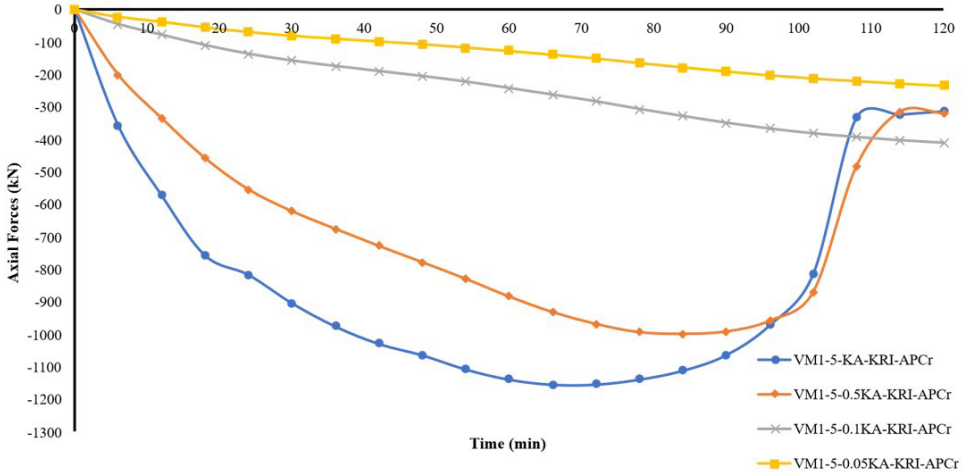

Figure 10 Results of the axial forces on the supports of composite beams with fire protection material SFRM Carboline type (VS 350x26 – 5 meters span) under different levels of axial restraint

Note that, in all the analyses, especially the models that have the highest axial stiffness, the beam presented lateral instability, explained by the compressive forces that arise in the beam due to its restriction on horizontal deformation and because they do not have any containment. The composite beams also presented lateral instability in the lower flange, in the region near to the supports (Figure 11). As the temperature increased, this instability spread to the entire beam. The appearance of this lateral instability in the composite beams is because the slab of the studied model is continuous, causing the greatest tensile forces to be in the upper part of the beam and the compression forces in the lower part to be gradually increased due to the restriction of axial expansion, besides the rotation restriction on the supports.

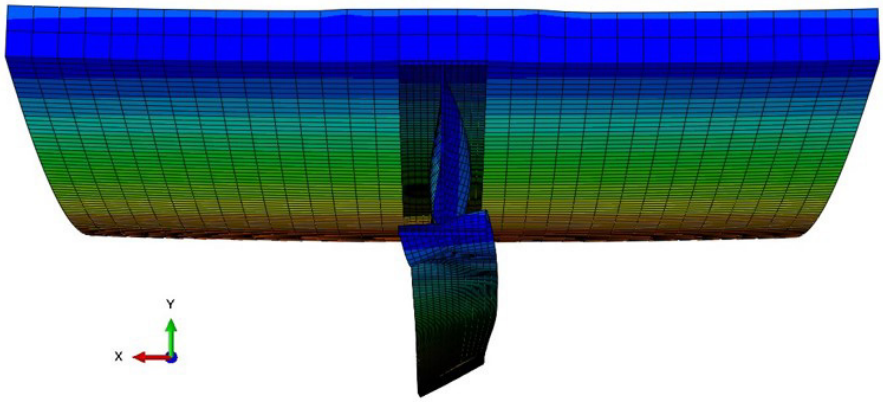

Figure 11 Lateral instability in models with highest axial stiffness

3.1.2 Influence of the distinction of fire protection coating materials

Figure 12 illustrate that all fire protection coating materials basically have the same value of axial compressive force and tension during the catenary action, except for the Carboline type, which does not present tension forces in 120 minutes of fire. The model without fire protection coating has a lower maximum compression axial force value than the fire protection models; however, it presented a greater tension force during the catenary action. This is because, without fire coating, temperatures develop rapidly in the steel beam, degrading the material before the beam can expand to its maximum value, accelerating vertical displacements. Another issue is that, with the reduction of axial stiffness, the maximum axial compressive forces decrease, whereas the tensile forces during catenary action remain at the same maximum value when compared to beams with greater axial stiffness. The reaction forces are thus verified to be a function

of the equilibrium of the structural element and not of the temperature when the beam is analyzed in isolation, although the different fire protection coatings present slight changes in the behavior of the beam. The beams were observed to only present tensile forces due to the action of catenary after the beam reaches the FRL (Fire Resistance Level), considering the mid-span displacement limit equal to L/30. This information is important, mainly for designing connections in a fire situation.

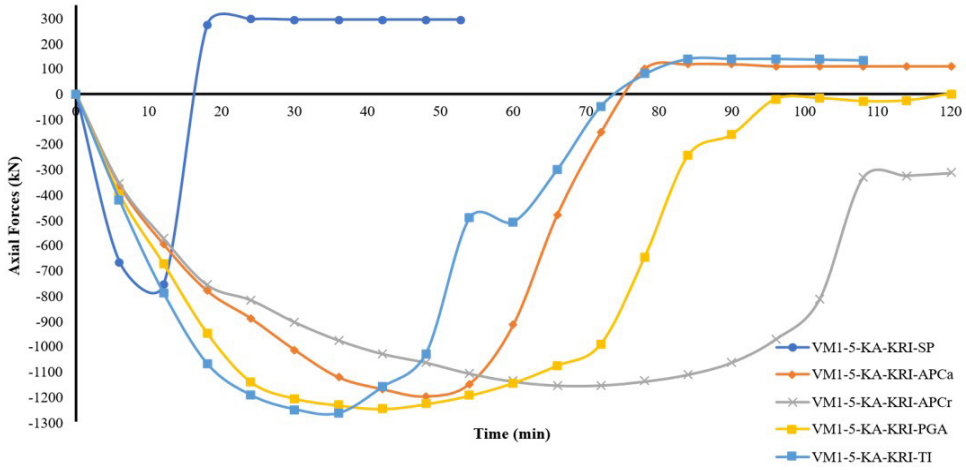

Figure 12 Results of axial forces on beam supports with varying fire protection material with full axial stiffness and infinite rotational stiffness (VS 350x26 – 5 meters span)

3.1.3 Influence of the span for fire protection coating beams

The influence of the span is present in Figure 13. The maximum compressive force shows to increase when the span is increased. The fire time in which the maximum compression force occurs also increases. This is explained by the reduction of the mass factor, since the greater the span is, the greater the cross-section of the beam, delaying the temperature distribution in the element.

For the 5- and 10-m span, only the beams coated with the SFRM Carboline type did not reach the catenary phase. However, for the span of 15 m, the square edged gypsum board does not reach the catenary phase in some levels of axial and rotational stiffness, leading to the conclusion that the occurrence of this effect also depends on the temperature distribution in the beam. Figures 14, 15 and 16 show the results of the axial forces of the beams by varying the spans for the other fire protection materials studied.

Finally, the same characteristics are found for the other types of fire protection coating studied and for the uncoated beams, showing that these compressive forces must be investigated with greater care. Another issue verified with the increase of spans of the beams was the change in behavior in relation to the variation of rotational stiffness. For the 5-meters span, the change in the level of rotational stiffness showed to have little influence on the results regarding axial forces. However, by increasing the beam span, decreased rotational stiffness caused variation in axial force. This occurs due to the large deformations of the beams in greater spans, since the beam moves more vertically before thermal expansion, responsible for the increase in axial forces. In composite beams, the rotation capacity of the connections can be concluded to have a direct influence on the axial forces generated by the elements surrounding the beams, more specifically the columns.

3.2 Effects of axial compression forces on columns in fire situation

To investigate the effects of axial compression forces on columns in fire situation because of the thermal expansion of the beams, the design of columns in fire situation was carried out with the insertion theses forces. With this, it will be evaluated if the force added to the column was preponderant to the design of these structural elements. First, a numerical study was carried out to determine the cross section of each column, based on the level of stiffness established in the parametric analysis.

For an axial force of 100 kN adopted here, equation $F = k.\delta$ (where “k” is the column stiffness and “δ” represents the displacement) allowed verifying the displacement that this force would generate for each stiffness studied. Then, the column cross sections that presented similar displacement values subjected to the same axial force of 100 kN were adopted, considering perimeter columns, with a length of 3 meters. Figure 17 shows the idealized model. Table 5 presents the cross sections of the columns considered for each level of axial stiffness for the beam spans of 5, 10 and 15 m, respectively. Brazilian CS-type sections (welded profile) were used, considering sections possible and feasible to connect the beam to the column flange.

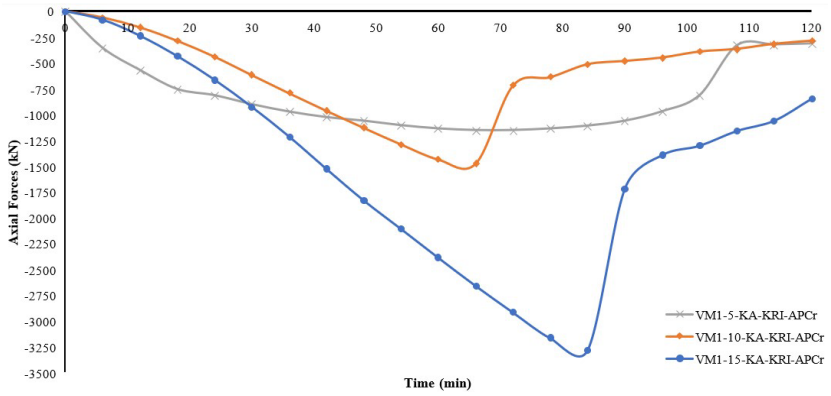

Figure 13 Results of the axial forces on the supports of composite beams with fire protection coating of the Carboline type for spans of 5, 10 and 15 meters, respectively

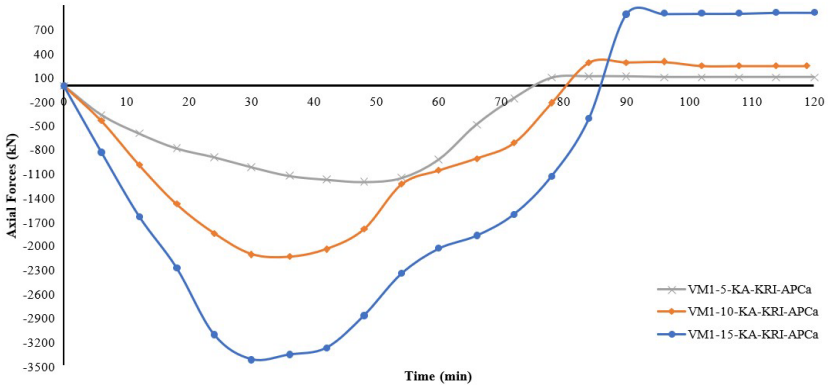

Figure 14 Results of the axial forces on the supports of composite beams with fire protection coating of the CACFO type for spans of 5, 10 and 15 meters, respectively

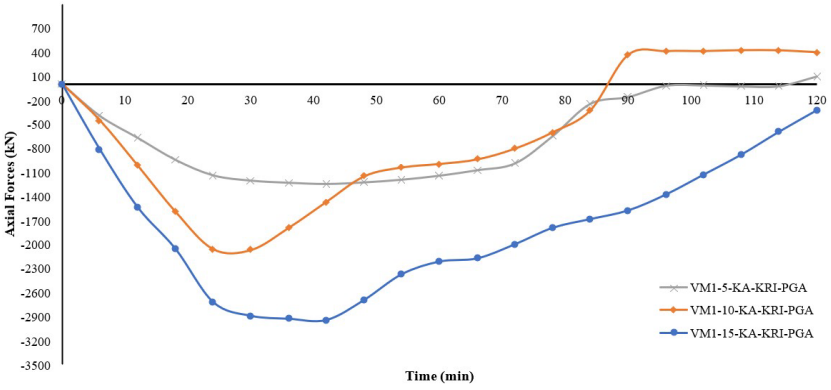

Figure 15 Results of the axial forces on the supports of composite beams with fire protection coating of the Square Edged Gypsum type for spans of 5, 10 and 15 meters, respectively

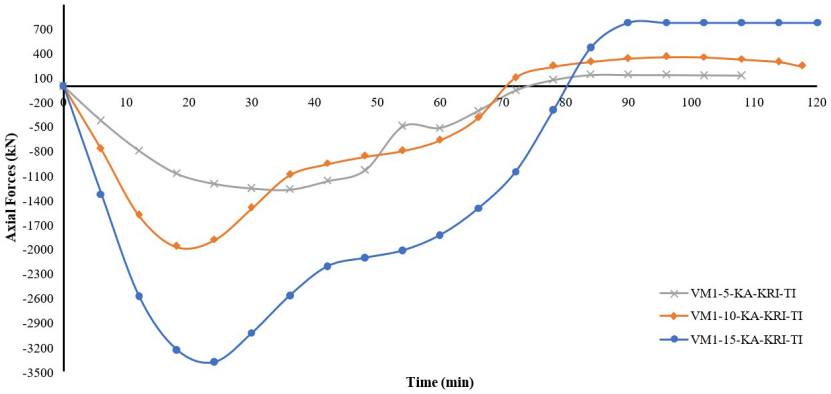

Figure 16 Results of the axial forces on the supports of composite beams with fire protection coating of the Intumescent Paint type for spans of 5, 10 and 15 meters, respectively

After determining the cross section, the resistance at room temperature was verified in accordance with ABNT NBR 8800 (Associação Brasileira de Normas Técnicas, 2008), considering that the section would be subjected to flexo-compression, and the loads used as the premise of this parametric analysis. Finally, the resistance of the column in a fire situation was verified according to ABNT NBR 14323 (Associação Brasileira de Normas Técnicas, 2013), considering the temperature of occurrence of the highest axial compression force to be transmitted to the columns as a bending moment (M_{sd} = F.L), where "F" is the force that appears due the thermal expansion of the beam, and "L" is the length of the column. Figure 18 depicts an interaction curve between bending moments and normal compression forces to exemplify the behavior of the resistance of a column in a fire situation, using the design equations of ABNT NBR 14323 (Associação Brasileira de Normas Técnicas, 2013), as given in the following equation 1:

$$\xi = \frac{N_{fi,Sd}}{N_{fi,Rd}} + \frac{M_{fi,x,Sd}}{M_{fi,x,Rd}} \leq 1.0 \quad (1)$$

where $N_{fi,Rd}$ and $M_{fi,Rd}$ are the design normal resistance and moment resistance in fire situation and Nfi,Sd e Mfi,Sd are the soliciting normal force and bending moment in fire situation.

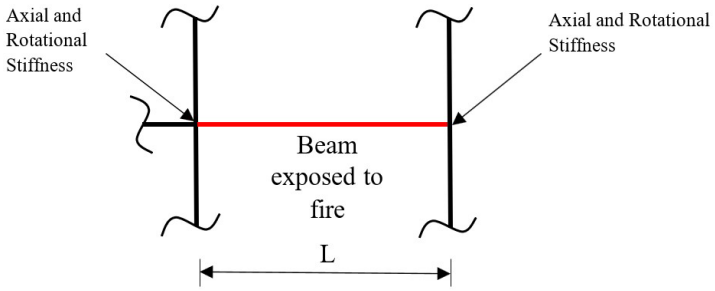

Figure 17 Representation of the idealized structural model

Table 5 Cross section of the columns chosen for analysis

Spam (m)	Axial Stiffness (kN/m)	Symbol	Cross Section
5	130800	KA	CS 450x154
5	67400	0.5KA	CS 400x106
5	13480	0.1KA	CS 250x51.8
5	6740	0.05KA	CS 200x38.8
10	184800	KA	CS 500x172
10	92400	0.5KA	CS 400x128
10	18480	0.1KA	CS 300x95
10	9240	0.05KA	CS 300x62.4
15	261067	KA	CS 550x228
15	130533	0.5KA	CS 450x154
15	26107	0.1KA	CS 400x106
15	13053	0.05KA	CS 350x93

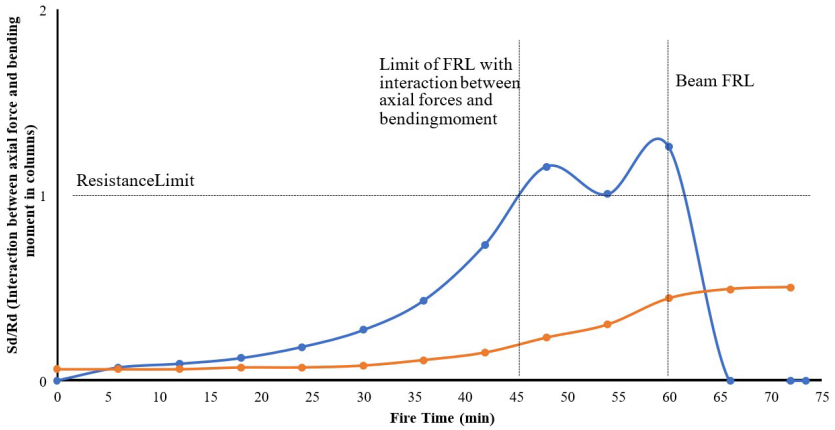

Figure 18 Interaction between axial force and bending moment in columns

In order to represent the design of columns in a fire situation, the model VM1-5-0.1KA-KRI-APCa (10% of the axial stiffness with SFRM CACFO300) was used, considering that the additional effects of the beams on the columns considerably changes the interaction between axial forces and bending moments. Considering the axial compressive forces that arise in beams with axial restraint, with approximately 45 minutes of fire, the column was observed to exceed its resistant capacity at high temperatures. However, the FRL of the beam analyzed is approximately 60 minutes (using the failure criterion for beam deformation equal to L/30). Observing the curve without interaction between the effects of the beam on the column, it is verified that, with the compressive and flexo-compression forces from the vertical loads only, the colum can have a FRL of 60 minutes, as well as the beam, causing an unsafe design in this specific case, if the buildings need to withsand 60 minutes of fire. In most cases, the columns with the largest cross section (greater stiffness to horizontal displacement) were found to serve to verify the interaction between bending moments (generated by the beam and the axial compression force of the beams) and axial forces. In this case, the main concern with the design must regard the axial compression forces that arise with the thermal expansion of the beams, since the normal stress had little influence, in the cases studied. However, in cases whereby the columns have a smaller cross-section, that is, with lower axial restrictions, the effect of the interaction between the forces can be unsafe for normative limits, even if the column is dimensioned at room temperature. Furthermore, in all the cases studied, the columns reach the resistance limit before the FRL established for the beam. Finally, by increasing the beam span, even the less slender columns were found not to meet the demands, since the axial forces that arise from beams with larger spans are considerably greater than those of smaller spans. A total of 60 cases were studied to investigate the effects of axial compression forces on column. The results of this study, considering only those found for the SFRM CACFO, are shown in table 6. From the table 6, “OK” refers to the situation that the design effect of actions for the fire situation is minor that the corresponding design resistance of the steel member, for the fire situation. “NOK” refers to the situation opposite to that exposed. Obviously, the study in question was limited to the evaluation of perimeter columns, not considering the structural elements working together, causing the efforts to be redistributed among the other members of the structure, especially in large displacements, a common characteristic of structures in fire situation.

Table 6 Column resistance verification in interaction with composite beams

Model	Time (min)	Max. Compression Force (kN)	Column Temperature	Interaction ξ	Verification
VM-5-KA	48	-1198	142	0.42	OK
VM-5-0.5KA	60	-1020	483	1.01	NOK
VM-5-0.1KA	76	-360.9	644	3.13	NOK
VM-5-0.05KA	78	-203.9	680	4.20	NOK
VM-10-KA	35	-2138	164	0.73	OK
VM-10-0.5KA	47	-1896.4	300	1.17	NOK
VM-10-0.1KA	72	-787.9	598	2.40	NOK
VM-10-0.05KA	78	-444.8	600	2.42	NOK
VM-15-KA	30	-3418	136	0.92	OK
VM-15-0.5KA	42	-3175	210	1.72	NOK
VM-15-0.1KA	75	-1645	486	1.81	NOK
VM-15-0.05KA	84	-1014	582	3.88	NOK

3.3 Effect of axial tensile forces on connections due to catenary action

To investigate the effects of the axial forces of the beams situation on the connections in fire situation due to the action of catenary, the first step was to choose the coated beam model with SFRM CACFO-300. This choice was because this numerical model presents a catenary action, with consequent axial tensile forces for all the spans studied. The rotation capacity in the supports related to the rotational restrictions considered in this parametric analysis was verified. A study of the Moment vs Rotation curve was carried out on the models of this work with total axial stiffness (KA) and varying the rotational stiffness (KR, 0.5KR, 0.1KR and 0.05KR) at room temperature, considering that the connections are coated, the temperature thus not influencing their behavior. The choice was based on the work by Andrade and Vellasco (2016), who present moment x rotation curves of several connections with different typologies. From the study of the moment x rotation curve of the beams (Figure 19), the following types of connections were designed for each value of rotational stiffness:

1. (1) KR → End plate (Figure 20a)
2. (2) 0.5KR → Top and seat angle with double web angle (Figure 20b)
3. (3) 0.1KR → Double web angle (Figure 20c)
4. (4) 0.05KR → Simple web angle (Figure 20d)

In this scenario, the effect of tensile axial forces on the connecting elements was evaluated, verifying whether the bolts and eventual welds were necessary. The number of bolts chosen was based on the criterion of the smallest number of bolts necessary to facilitate the drilling template of the connections in the execution. The bolts used are ASTM A325 type (Fu = 825 MPa). The fillet weld was used, with an 8-mm long vertical leg and E70 electrode. Finally, the diameter of the bolts chosen was the one that met all the requests at room temperature. The connections verification was carried out with ABNT NBR 8800 (Associação Brasileira de Normas Técnicas, 2008) criteria for interaction between shear and tensile forces in the connections elements, as given in the following equation (2):

$$\left(\frac{F_{t,Sd}}{F_{t,Rd}}\right)^2 + \left(\frac{F_{v,Sd}}{F_{v,Rd}}\right)^2 \leq 1.0 \tag{2}$$

where $F_{t,Rd}$ and $F_{v,Rd}$ are the tensile and shear resistance of the connecting element and Ft,Sd and Fv,Sd are the tensile and shear forces in the connecting element.

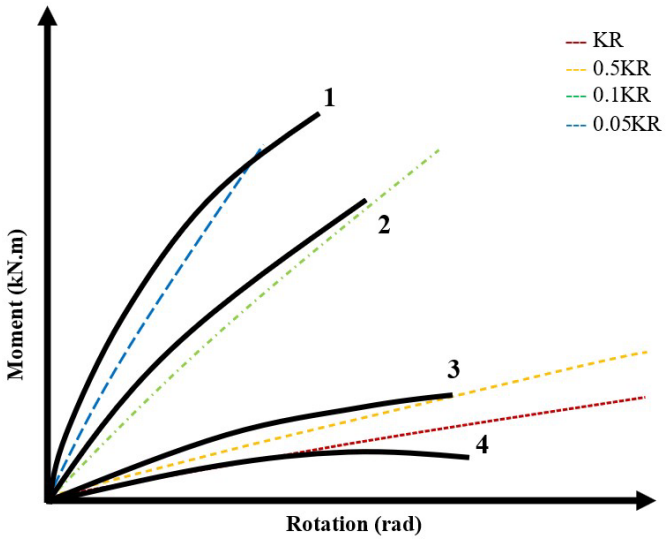

Figure 19 Moment-Rotation curve of the connections (Andrade and Vellasco, 2016 – Adapted)

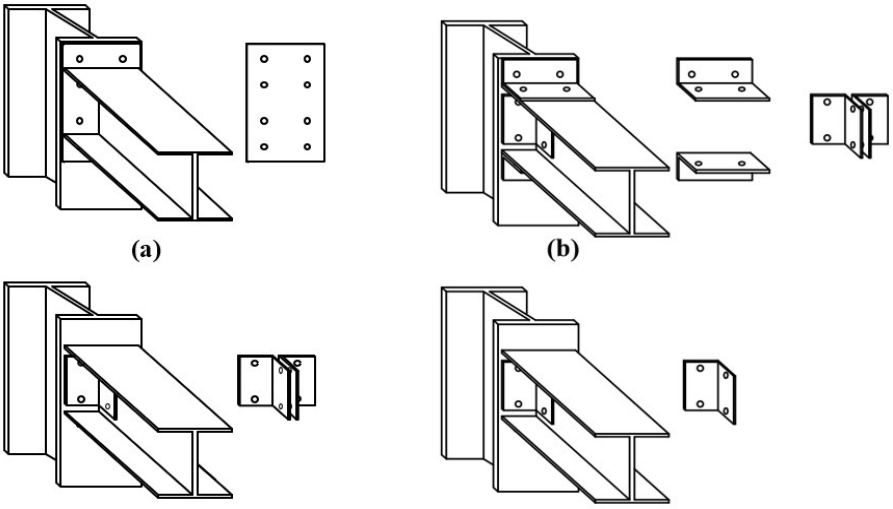

Figure 20 Typology of connections

To determine the temperature in the connections, the method provided for in Annex D, item D.3 of Eurocode 3 Part 1-2 (2005) was used, which correlates the temperature at the height of the steel beam, next to the joint, with the temperature at the lower table in the center of the beam span.

From the results, the connections are verified to suffer little influence due to the catenary action, with only a few numerical models with unsafe resistance to efforts in a fire situation. Most of the 0.1KR and 0.05KR models (10% and 5% of the beam rotational stiffness value, respectively) were found to have values greater than the resistance of the connection. This thus indicates that the use of this type of joint in a fire situation must be carefully checked, so that there is no collapse in the connections. However, also note that in all the models without fire protection coating, the connections fail according to normative criteria, as soon as the beam enters the catenary phase, showing that the tensile forces are predominant in this case and that the joint elements must always be coated against fire. Table 6 show the results of this study, considering only those found for the SFRM CACFO.

Finally concluded was that the verification of connections in a fire situation can be neglected (except for the joint proposed for the 0.1KR and 0.05KR models, as already highlighted) if they are coated against fire, following the recommendation provided in ABNT NBR 14323 (Associação Brasileira de Normas Técnicas, 2013). In the specific cases shown, which do not meet the requirements in a fire situation, the recommendation is to design the connections using the temperature distribution in the joint elements provided in Annex D of Eurocode 3 Part 1-2 (11). Also advisable is to evaluate the value of tensile axial force in the catenary phase for designing connections in fire situation; the equation in Allam et al. (2002) and Guo et al (2018) can be used to predict the tensile forces.

4 CONCLUSION

This paper contributed with studies on the behavior of restrained fireproof composite beams and the interaction that these restraints have with the elements surrounding the beam. The parametric study covered four different fire protection coating materials, axial and rotational constraint level, and beam span variation. Based on the simulation results, the following conclusions can be drawn:

- The variation in rotational constraint has little influence on beams with small spans. By increasing the span of the beams and, consequently, their vertical displacements, the rotational stiffness starts to present a preponderant influence, mainly on the axial compression forces.
- The different types of fire protection coating of the beams studied present the same values of axial compression and tensile forces in the catenary phase, although the fire time for the appearance of each of these forces is different. The reaction forces are verified to be a function of the equilibrium of the element and not of the temperature, considering the isolated beam.
- The variation in the span of the beams influences the axial forces, both of compression and tensile in the action of the catenary. Therefore, the greater the span of the beam is, the greater its support reaction. However, beams with larger spans present their maximum compressive forces in longer fire times, being harmful to the column, since the higher the temperature in the structural element is, the lower its resistance.

- In the analysis of the interaction between the beams and columns, considering these columns as considered unbraced external columns, it was found that, if the beams are coated and the columns are not, they will all fail due to the compressive forces, and due to the restriction on axial expansion.
- The recommendation is that the compressive force that arises because of beam expansion and axial restraint is carefully evaluated so that columns in fire situation consider the bending moments caused by this force.
- Regarding the compressive forces that emerged, it is worth mentioning that the analysis was carried out in isolated beams in a fire situation, without considering the effects of the redistribution of efforts when the beams and columns are inserted in frames.
- Except in specific cases, the connections were verified not to be the weakest point of the structure in a fire situation, if they are coated against fire. In most cases of parametric analysis, the values of axial tensile forces that arise in the catenary phase of the beam were found not to be sufficient for the connections to fail, if they are perfectly dimensioned at room temperature.
- he greatest axial tensile forces in the catenary action of the beam were observed to only appear after the FRL of the beam. Thus, such forces would only appear if the fire lasts longer than the fire resistance time of the structural element. However, this situation would not occur if the beams and connections were not coated, since the decrease.

Acknowledgments

The main author thanks the Brazilian Air Force for allowing his doctoral studies. Grant 2018/14735-6, São Paulo Research Foundation (FAPESP) and Conselho Nacional de Pesquisa e Desenvolvimento Científico (CNPq).

Author's Contribuitions: Conceptualization, ICS Leite; Methodology, ICS Leite; Investigation, ICS Leite; Writing - original draft, ICS Leite; Writing - review & editing, ICS Leite and V P Silva; Funding acquisition, VP Silva; Resources, ICS Leite and VP Silva; Supervision, VP Silva.

Editor: Pablo Andrés Muñoz Rojas

References

Allam, A. M., Burgess, I. W., & Plank, R. J. (2002). Performance-based simplified model for a steel beam at large deflection in fire. In Proc. 4th International Conference on Performance-Based Codes and Fire Safety Design Methods, Melbourne, Australia.

Allam, A., Nassif, A., & Nadjai, A. (2019). Behaviour of restrained steel beam at elevated temperature–parametric studies. Journal of Structural Fire Engineering, 10(3), 324-339.

Andrade, S., & Vellasco, P. (2016). Comportamento e projeto de estruturas de aço. Elsevier Brasil.

Associação Brasileira de Normas Técnicas (2014). NBR 6118 Design of concrete structures - Procedure, Rio de Janeiro, Brazil.

Associação Brasileira de Normas Técnicas (2008). NBR 8800 Design of steel and composite structures for buildings, Rio de Janeiro, Brazil.

Associação Brasileira de Normas Técnicas (2013). NBR 14323 Structural fire design of steel and composite steel and concrete structures for buildings, Rio de Janeiro, Brazil.

Cedeno, G. A., Varma, A. H., & Gore, J. (2011). Predicting the standard fire behavior of composite steel beams. In Composite construction in steel and concrete VI (pp. 642-656).

Chen, L., & Wang, Y. C. (2012). Efficient modelling of large deflection behaviour of restrained steel structures with realistic endplate beam/column connections in fire. Engineering Structures, 43, 194-209.

EN 1993-1-2. (2005). Design of steel structures—part 1-2: general rules—structural fire design. Eurocode 3.

Guo, Z., Gao, R., Zhang, X., & Jia, X. (2018). Fire Resistances of Restrained Steel Beams Subjected to Fire Loads. KSCE Journal of Civil Engineering, 22, 3028-3038.

Jankowiak, T., & Lodygowski, T. (2005). Identification of parameters of concrete damage plasticity constitutive model. Foundations of Civil and Environmental Engineering, 6(1), 53-69.

Kodur, V. K. R., & Dwaikat, M. M. S. (2009). Response of steel beam–columns exposed to fire. Engineering Structures, 31(2), 369-379.

Kodur, V. K. R., & Shakya, A. M. (2013). Effect of temperature on thermal properties of spray applied fire resistive materials. Fire Safety Journal, 61, 314-323.

Krishnamoorthy, R. R. (2011). The analysis of partial and damaged fire protection on structural steel at elevated temperature. The University of Manchester (United Kingdom).

Leite, I. C. S. and Silva, V. P. (2021) “Analise termestrutural de vigas de aco com a utilizacao da ferramenta computacional abaqus,” Anais do XII Congresso Brasileiro de Pontes e Estruturas.

Liu, T. C. H., Fahad, M. K., & Davies, J. M. (2002). Experimental investigation of behaviour of axially restrained steel beams in fire. Journal of Constructional Steel Research, 58(9), 1211-1230.

Martinez, J., & Jeffers, A. E. (2021). Analysis of restrained composite beams exposed to fire. Engineering Structures, 234, 111740.

Najafi, M. (2014). Behaviour of Axially Restrained Steel Beams with Web Openings at Elevated Temperatures. The University of Manchester (United Kingdom).

Rigobello, R. (2011). Desenvolvimento e aplicação de código computacional para análise de estruturas de aço aporticadas em situação de incêndio (Doctoral dissertation, Universidade de São Paulo).

Romagnoli, L. C., & Silva, V. P. (2020). Numerical analysis of composite steel and concrete beams subjected to fire under different support conditions. Revista IBRACON de Estruturas e Materiais, 13.

Selden, K. L. and Varma, H. A. (2016). Composite beams under fire loading: numerical modeling of behavior. Journal of Structural Fire Engineering, Vol. 7, Iss 2, 142-157.

Silva, V. P. (1997). O Incêndio e as Estruturas de Aço. Estruturas de aço: conceitos, técnicas e linguagem.

Usmani, A. S., Rotter, J. M., Lamont, S., Sanad, A. M., & Gillie, M. (2001). Fundamental principles of structural behaviour under thermal effects. Fire Safety Journal, 36(8), 721-744.

Wainman, D. E., & Kirby, B. R. (1987). Compendium of UK standard fire test data, unprotected structural steel–1. Ref. No (Vol. 10328, pp. 1-26). RS/RSC.

Wang, Y. C. (2002). Steel and composite structures: behaviour and design for fire safety. CRC Press.

Yin, Y. Z., & Wang, Y. C. (2004). A numerical study of large deflection behaviour of restrained steel beams at elevated temperatures. Journal of Constructional Steel Research, 60(7), 1029-1047.